Supporting Information

Li et al. 10.1073/pnas.1109773109

SI Materials and Methods

Cell Culture and Preparation of Primary Islet β Cells. All the culture media contained penicillin (100 U/mL) and streptomycin (100 μg/mL). INS-1 cells were cultured in RPMI 1640 medium (Gibco, with 11.1 mM glucose) supplemented with 10% (vol/vol) FBS, 2-mercaptoethanol (50 μM), sodium pyruvate (1 mM), L-glutamine (2 mM), and Hepes (10 mM). MIN6 cells were cultured in high-glucose DMEM (Gibco) containing 10% (vol/vol) heat-inactivated FBS and 2-mercaptoethanol (3.5 μL for 1 L of medium). Cells were grown in 5% (vol/vol) CO_2 at 37 °C and passed by trypsinization when they reached >80% confluence. The culture medium was changed every 2–3 d.

Primary β cells were prepared from dispersed islets. We typically incubated ∼100–500 islets in 1 mL of Accutase solution (catalog no. AT-104; Innovative Cell Technologies) for 15 min at 37 °C and gently pipetted cells up and down 15–20 times to promote dissociation. Digestion was stopped by adding 9 mL of culture medium, and cells were collected by centrifugation at 300 × *g* for 5 min. Dissociated islet cells were then resuspended in the culture medium and seeded in imaging dishes. Rodent islet cells were cultured in RPMI 1640 supplemented with 10% (vol/vol) heat-inactivated FBS. Human islet cells were cultured in CMRL medium (Mediatech, Inc.) supplemented with 10% (vol/vol) FBS and glucose (final concentration of 10 mM).

Islets from ZnT8 WT and KO animals were prepared as described elsewhere (1). Pancreatic islets were allowed to recover overnight in culture medium and were dissociated by incubation in Hanks'-based enzyme-free cell dissociation buffer for 10 min at room temperature before centrifugation and gentle pipetting (1). Dissociated cells were plated onto 24-mm sterile coverslips and allowed to recover overnight before imaging.

ZIMIR Imaging by Wide-Field Fluorescence Microscopy. Wide-field fluorescence microscopy was carried out on an inverted fluorescence microscope (Axiovert 200; Carl Zeiss) equipped with a cooled CCD camera (ORCA-ER; Hamamatsu). Cells to be imaged were seeded on 35-mm imaging dishes with glass bottoms (catalog no. P35G-0-10-C; MatTek) at 30–40% confluence. During imaging, cells were excited with light from a 175-W xenon lamp after passing through appropriate band-path filters (2) and an objective with a magnification of 40×. Hardware automation, image acquisition, and image analysis were carried out with Openlab imaging software (Perkin–Elmer).

To characterize the response of membrane-anchored ZIMIR to changes of $[Zn^{2+}]_e$, we varied $[Zn^{2+}]_e$ from low nanomolar to micromolar, using Zn^{2+} buffers containing NTA (for $[Zn^{2+}]_e <$ 100 nM) (3) or histidine (for $[Zn^{2+}]_e \geq 100$ nM) (4). After recording fluorescence images at different $[Zn^{2+}]_e$ levels, we washed cells with a nominally Zn^{2+}-free SAB containing 0.2 mM DPAS and followed the decay of ZIMIR fluorescence intensity along the plasma membrane.

Most cell imagings were performed in a secretion assay buffer (SAB) containing 114 mM NaCl, 4.7 mM KCl, 1.2 mM KH2PO4, 2.5 mM CaCl2, 1.16 mM MgSO4, 3 mM glucose, and 20 mM Hepes (pH 7.4). After image acquisition, membrane ZIMIR fluorescence intensity was measured by drawing regions of interest along the plasma membrane, and its time course was normalized against its baseline value after background subtraction [i.e., (F - Fbkg)/(F0 - Fbkg), where Fbkg is the average background fluorescence intensity of a nearby area containing no cells].

To image zinc release in islets extracted from ZnT8 WT and KO animals, we labeled dissociated islets with ZIMIR (final concentration of 2 μM plus pluronic) in Krebs Hepes-bicarbonate Buffer [KHB; containing 140 mM NaCl, 3.6 mM KCl, 0.5 mM NaH_2PO_4, 0.2 mM $MgSO_4$, 1.5 mM $CaCl_2$, 10 mM Hepes (pH 7.4), 2 mM $NaHCO_3$] preequilibrated with 95:5 O_2/CO_2. Dissociated islets were then washed twice before imaging on an Olympus IX-70 using a 40× oil immersion objective and an Imago CCD camera (Till Photonics) controlled by TILLvislON software (Till Photonics). Dissociated islet cells were maintained at 37 °C throughout using a heating stage (MC60, LINKAM; Scientific Instruments), and KHB buffer was perifused (1 mL/min) with the additions marked on figures. During glucose (17 mM) stimulation, we also included forskolin (1 μM) and 3-isobutyl-1-methylxanthine (5 μM). Images were acquired at 1 Hz using a 100-ms exposure time and a 488-nm excitation wavelength. We used a monochromator (Polychrome IV; Till Photonics), and the emission signals were detected at 515 nm.

Islet Isolation and Preparation of Primary β Cells from Dissected Islets. Experiments with rodents were carried out according to protocols approved by the Institutional Animal Care and Use Committee of University of Texas Southwestern Medical Center or by the UK Home Office Animal Scientific Procedure Act (1986). Rodent islets were isolated from Sprague–Dawley rats or C57BL/6 mice after digesting exocrine tissues of pancreas using collagenase (5). Briefly, young adult animals 12–20 wk old were anesthetized by i.p. injection of Nembutal and killed by cervical dislocation. The internal organs were exposed after abdominal incision. After clamping the ampulla on the duodenum wall, we perfused the pancreas with ∼4 mL of collagenase solution (Roche Collagenase P, catalog no. 11213857001; 1.4 mg/mL dissolved in HBSS). The pancreas was then digested in another 1 mL of collagenase solution at 37 °C for ∼15 min. When the digestion suspension became homogeneous and appeared milky, we stopped the digestion by leaving the tube on ice and adding 14 mL of cold HBSS. Cells were centrifuged at 250 × *g* for 2 min. Supernatant was decanted, and cells were resuspended in 10 mL of HBSS. After repeating the process one more time, we hand-picked the resuspended islets using a pipette under a dissection scope. Isolated rodent islets were cultured at 37 °C with 5% (vol/vol) CO_2 in RPMI medium 1640 containing 10% (vol/vol) FBS.

Human islets were obtained through the Integrated Islet Distribution Program sponsored by the National Institute of Diabetes and Digestive and Kidney Diseases and the Juvenile Diabetes Research Foundation International, and they were shipped to us from the sponsored islets' isolation centers at the Scharp/Lacy Institute, University of Pennsylvania, University of Miami, University of Wisconsin, and Southern California Islet Consortium. Human islets were cultured at low density (1,000 islets eq/mL) in CMRL medium supplemented with 10% (vol/vol) FBS and glucose (final concentration of 10 mM) in 5% (vol/vol) CO_2. On receiving human islets, we first incubated them at 37 °C overnight before culturing them at 25 °C.

Immunohistochemical Labeling of α and β Cells After ZIMIR Imaging. After ZIMIR imaging, islets were rinsed twice with ice-cold PBS [137 mM NaCl, 2.7 mM KCl, 8 mM Na_2HPO_4, 2 mM KH_2PO_4 (pH 7.3)] and fixed with 4% (wt/vol) formaldehyde (diluted from BP531-500 in PBS; Fisher) at room temperature (RT) for 30 min. Islets were then permeabilized with Triton X-100 [1% (vol/vol) in PBS] at RT for 30 min, washed three times with PBS (5 min each), blocked with 1% BSA and 1.7% (wt/vol) goat serum for 40 min at RT, and incubated with primary antibodies against

insulin (1:50 dilution of guinea pig anti-human insulin, catalog no. 4011-01F; Millipore) and glucagon (1:3,000 dilution of mouse antiglucagon; catalog no. G2654; Sigma) at 4 °C overnight. The solution was decanted the following day, and the islets were washed three times (for 5 min each wash) with ice-cold PBS. We then added secondary antibodies (1:50 dilution of FITC-labeled anti-guinea pig, catalog no. 106-095-003 and 1:2,000 dilution of Cy3 labeled anti-mouse, catalog no. 111-165-144; both from Jackson) and incubated islets at RT for 1 h. After washing islets three times with ice-cold PBS, we acquired confocal images in both FITC and Cy3 channels in a 1-μm z-step using an LSM510 confocal laser scanning microscope (Carl Zeiss). During the entire procedure, care should be taken to minimize agitation and to avoid islets from detaching off the glass coverslip.

Concurrent Electrophysiological Recording and ZIMIR Imaging. Electrophysiological recordings and stimulation were done in standard whole-cell configuration using an EPC9 patch-clamp amplifier controlled by Pulse acquisition software (HEKA Elektronik). The pipette solution contained 10 mM NaCl, 125 mM Cs-glutamate, 10 mM KCl, 1 mM $MgCl_2$, 5 mM Hepes (pH 7.15 with CsOH), 3 mM MgATP, and 0.1 mM cAMP. The extracellular bath solution contained 120 mM NaCl, 4.8 mM KCl, 24 mM $NaHCO_3$ (saturated with CO_2), 5 mM Hepes (pH 7.4 with NaOH), 0.5 mM NaH_2PO_4, 1.5 mM $CaCl_2$, 0.5 mM $MgSO_4$, 0.01 mM EDTA, and 3 mM glucose. The experiments were conducted at 33 °C using dissociated primary islet β cells from female CD-1 mice. After islet isolation and dissociation, cells were plated on glass coverslips and cultured for >24 h before the assay.

The imaging experiments were done on an Olympus IX-71 microscope with a UPlanFL N objective with a magnification of 40× (Olympus). For acquisition, an F-View-ll camera and MT-20 excitation system equipped with an Hg arc lamp were used, under control of Cell ^ R software (all from Olympus). The dye was excited at 490 nm, and emission at 530 nm was recorded. Images were acquired at a frequency of 0.5 Hz with typical excitation times of 10 ms. The acquisition of the fluorescence and electrophysiological data was synchronized using the transistor–transistor logic (TTL) pulse.

After establishing the standard whole-cell configuration, series resistance and cell capacitance were compensated for automatically by the acquisition software. Recordings, triggered by the TTL pulse from the imaging software, were started in current-clamp mode, after which the cell was voltage-clamped at −70 mV to allow the equilibration of the solution between the cell and the pipette. The depolarization-induced changes in the cell capacitance were then recorded using the "Sine + DC" method implemented in the acquisition software. The cell was held at −70 mV and subjected to 10 depolarizing 2.5-s pulses to 0 mV following at a 0.5-s interval during which a 500-Hz, 30-mV sinusoid was applied (as shown in Fig. S2). Electrophysiological data were filtered at 10 kHz, digitized at 20 kHz, and further combined with imaging data and analyzed using Igor Pro software (Wavemetrics).

Synthesis. All reagents were purchased from Aldrich or VWR. Anhydrous solvents were stored over activated molecular sieves (3 Å or 4 Å). TLC was performed on precoated silica gel 60F-254 glass plates (EM Science). Reaction products were purified by low-pressure flash chromatography (FC) using silica gel 60 (63–200 μm; EM Science). ^{1}H-NMR spectra were acquired on a Varian 400-MHz or 500-MHz spectrometer. Chemical shifts (δ, ppm) were reported against tetramethylsilane (0 ppm). MALDI-TOF MS was performed on a Voyager-DE PRO biospectrometry workstation (Applied Biosystems) using 2,5-dihydroxy benzoic acid as the matrix.

2-[Bis(2-pyridinylmethyl)amino]-ethanesulfonic acid (DPAS) (6), 2-pyridylmethyl-[2-(2-pyridyl)ethyl]amine (compound 5) (7), and *N*-ethyl glycine methyl ester or *N*-dodecyl glycine ethyl ester (8) were prepared according to the published procedures.

Preparation of 6-Nitro-4′,5′-Dimethylfluorescein Dipivaloyl Ester (Compound 1). 4-Nitrophthalic acid anhydride (0.97 g, 5.0 mmol) and 2-methyl resorcinol (1.30 g, 10.5 mmol) were suspended in 100 mL of methanesulfonic acid. The mixture was stirred at 80 °C for 8 h. After cooling, the reaction was quenched in 100 mL of ice water and the mixture was passed through a sintered glass filter. The retentate was dried under vacuum at 50 °C for 8 h. The resulting dark red solid was then added to a suspension of Cs_2CO_3 (3.58 g, 11 mmol) in dimethylformamide (DMF, 20 mL). To this solution was added 2.24 mL of pivalic anhydride. Two hours later, the reaction mixture was filtered and the residue was washed with MeOH (20 mL). The filtrate was evaporated, and the resulting residue was extracted with $CHCl_3$ (3 × 50 mL) and saturated brine. The organic layer was dried over Na_2SO_4, concentrated, and purified by FC (hexane/EtOAc, 20:1–4:1) to provide the product (5-nitro isomer; 0.607 g, 21.2%), the 6-nitro isomer (0.780 g, 27.2%), and the mixture of both isomers (1.338 g, 46.7%) as white solids.

5-Nitro-4′,5′-dimethylfluorescein dipivaloyl ester: ^{1}H NMR ($CDCl_3$, 400 MHz): δ 8.86 [doublet (d), J = 2.0 Hz, 1H], 8.52 [doublet of doublet (dd), J = 2.0, 8.4 Hz, 1H], 7.37(d, J = 8.4 Hz, 1H), 6.76 (d, J = 8.8 Hz, 2H), 6.64 (d, J = 8.8 Hz, 2H), 2.34 [singlet (s), 6H], 1.40 (s, 18H). MS was performed: 573.20 calculated for $C_{32}H_{31}NO_9$; observed: 574.57 $(M + H)^+$, 596.52 $(M + Na)^+$.

6-Nitro-4′,5′-dimethylfluorescein dipivaloyl ester (compound 1, Fig. S1): ^{1}H NMR ($CDCl_3$, 400 MHz): δ 8.47 (dd, J = 2.0, 8.4 Hz, 1H), 8.20 (d, J = 8.4 Hz, 1H), 8.00 (d, J = 2.0 Hz, 1H), 6.76 (d, J = 8.8 Hz, 2H), 6.65 (d, J = 8.8 Hz, 2H), 2.35 (s, 6H), 1.40 (s, 18 H). MS was performed: 573.20 calculated for $C_{32}H_{31}NO_9$; observed: 574.57 $(M + H)^+$, 596.52 $(M + Na)^+$.

Preparation of 6-Nitro-4′,5′-Dibromomethylfluorescein Dipivaloyl Ester (Compound 2). Compound 1 (57.4 mg, 0.10 mmol) mixed with *N*-bromosuccinimide (55.2 mg, 0.31 mmol) and benzoyl peroxide (10 mg) in CCl_4 (10 mL) was refluxed for 4 h. The mixture was cooled and filtered, and the solid residue was washed with Et_2O. The filtrate was concentrated and purified by FC (hexane/EtOAc, 10:1–8:1) to afford compound 2 (72 mg, 98.4%): ^{1}H NMR ($CDCl_3$, 400 MHz): δ 8.52 (dd, J = 2.0, 8.4 Hz, 1H), 8.24 (d, J = 8.4 Hz, 1H), 8.07 (d, J = 2.0 Hz, 1H), 6.93 (d, J = 8.8 Hz, 2H), 6.80 (d, J = 8.8 Hz, 2H), 4.80 (d, J = 2.4 Hz, 4H), 1.44 (s, 18 H). MS was performed: 731.02 calculated for $C_{32}H_{29}Br_2NO_9$; observed: 732.35 $(M + H)^+$.

Preparation of 2,2-Dimethoxy-*N*-[2-(2-pyridinyl)ethyl]-*N*-(2-pyridinylmethyl)-Aminoethane (6 and 7). These compounds were prepared based on a known procedure (9). Compound 5 (0.646 g, 3.03 mmol) (7) was mixed with 2-bromo-1,1-dimethoxyethane (1.44 mL, 12.12 mmol), Na_2CO_3 (3.21 g, 30.3 mmol), and potassium fluoride/celite (1:1, 240 mg) in 18 mL of acetonitrile. The mixture was refluxed for 3 d under argon, cooled, and filtered. The solid residue was washed with CH_3CN. The filtrate was concentrated and purified by FC (dichloromethane/MeOH, 50:1–20:1) to afford compound 6 (0.542 g, 59%) as a yellow oil: ^{1}H NMR ($CDCl_3$, 400 MHz): δ 8.51 (m, 2H), 7.60 (dd, J = 7.6, 2.0 Hz, 2H), 7.37 (d, J = 7.6 Hz, 1H), 7.11 (m, 3H), 4.46 [triplet (t), J = 5.2 Hz, 1H], 3.93 (s, 2H), 3.32 (s, 6H), 3.05 [4H, multiplet (m)], 2.80 (2H, d, J = 5.6 Hz). MS was performed: 301.18 calculated for $C_{17}H_{23}N_3O_2$; observed: 302.46 $(M + H)^+$.

The above intermediate 6 (0.344 g, 1.14 mmol) was suspended in an aqueous 1-N HCI solution (16 mL) and stirred at RT for 6 h. The solvent was removed under vacuum, and the residue was

dried under a high vacuum overnight to provide the product (compound 7) as a yellow solid (0.482 g): ^{1}H NMR (D_4-MeOH, 400 MHz): δ 8.95 (d, J = 6.0 Hz, 1H), 8.67(dd, J = 6.0, 0.8 Hz, 1H), 8.05 (d, J = 8.4 Hz, 1H), 7.96 (t, J = 6.8 Hz, 1H), 7.88 (m, 2H), 6.05 (t, J = 4.4 Hz, 1H), 4.36 (s, 2H), 3.45–3.37 (m, 4H), 3.18 (m, 2H). MS was performed: 256.14 calculated for $C_{15}H_{18}N_3O^+$; observed: 256.34 M^+.

Preparation of Compound 3. A mixture of compound 2 (33.6 mg, 46 μmol), NaI (13.8 mg, 92 μmol), *N*-ethyl glycine methyl ester (184 μmol), and proton sponge (20 mg, 92 μmol) in anhydrous acetonitrile (1.0 mL) was fluxed overnight. The solution was concentrated, and the residue was purified by FC (hexane/EtOAc, 20:1–2:1) to yield the product compound 3a as a yellow oil (96%): ^{1}H NMR ($CDCI_3$, 400 MHz): δ 8.46 (dd, J = 1.8, 8.4 Hz, 1H), 8.18 (d, J = 8.4 Hz, 1H), 8.08 (d, J = 1.8 Hz, 1H), 6.75 (s, 4H), 4.18 (m, 4H), 3.58 (s, 6H), 3.47 (s, 4H), 2.84 (quartet, J = 7.2 Hz, 4H), 1.37 (s, 18H), 1.02 (t, J = 7.2 Hz, 6H).

Compound 3b was prepared similarly from compound 2 and *N*-dodecyl glycine ethyl ester in 78% yield: ^{1}H NMR ($CDCI_3$, 400 MHz): δ 8.46 (dd, J = 2.0, 8.4 Hz, 1H), 8.17 (d, J = 8.4 Hz, 1H), 8.03 (d, J = 2.0 Hz, 1H), 6.75 (s, 4H), 4.18 (m, 4H), 4.04 (m, 4H), 3.46 (s, 4H), 2.74 (t, J = 7.4 Hz, 4H), 1.38 (s, 18H), 1.20 (m, 46H), 0.86 (t, J = 7.4 Hz, 6H). MS was performed: 1,111.67 calculated for $C_{64}H_{93}N_3O_{13}$; observed: 1,112.32 $(M + H)^+$.

Preparation of Compound 4. To a solution of compound 3a (84 μmol) in MeOH/THF/H_2O (4:1:1, 6 mL) was added sodium hydrosulfide hydrate (400 mg, 68%). The mixture was refluxed for 1.5 h. The solvent was concentrated under vacuum, and the residue was purified by reversed phase column chromatography (LiChroprep RP-18, EMD Chemicals) to yield the product (compound 4a) as a red solid (81%): ^{1}H NMR (D_4-MeOH, 400 MHz): δ 7.88 (d, J = 8.4 Hz, 1H), 7.07 (d, J = 9.6 Hz, 2H), 6.80 (dd, J = 2.4, 8.8 Hz, 1H), 6.51 (d, J = 9.2 Hz, 2H), 6.41 (d, J = 2.4 Hz, 1H), 4.01 (m, 2H), 3.85 (m, 2H), 3.18–3.35 (m, 4H), 3.15–2.75 (m, 4H), 1.17 (t, J = 7.2 Hz, 6H). MS was performed: 577.21 calculated for $C_{30}H_{31}N_3O_9$; observed: 578.16 $(M + H)^+$.

Compound 4b was prepared similarly from compound 3b in 74% yield: ^{1}H NMR (D_4-MeOH, 400 MHz): δ 7.84 (d, J = 8.8 Hz, 1H), 7.15 (d, J = 9.2 Hz, 2H), 6.80 (dd, J = 2.4, 8.4 Hz, 1H), 6.53 (d, J = 9.2 Hz, 2H), 6.39 (d, J = 2.4 Hz, 1H), 4.64 (m, 4H), 3.65 (m, 4H),3.25 (m, 4H), 1.83 (m, 4H), 1.20–1.45 (m, 36H), 0.88 (m, 6H). MS was performed: 857.52 calculated for $C_{50}H_{71}N_3O_9$; observed: 858.11 $(M + H)^+$, 615.21 $(M\text{-}C_{14}H_{28}NO_2)^+$, 372.22 $(M\text{-}C_{28}H_{57}N_2O_4)^+$.

Preparation of ZIMIR-C_2 and ZIMIR. The general procedure of preparing ZIMIRs involves mixing compound 4 with 3 eq of compound 7 in anhydrous MeOH containing dried Na_2SO_4 (100 eq). The mixture was stirred at RT for several hours under argon. $NaCNBH_3$ (5 eq) was then added. The reaction was continued overnight, and the mixture was filtered. The filtrate was concentrated, and the resulting residue was purified by reversed phase column chromatography (LiChroprep RP-18). ZIMIR-C_2 was obtained as a red film in 36% yield: ^{1}H NMR (D_4-MeOH, 400 MHz): δ 8.33 (t, J = 6.0 Hz, 2H), 7.86 (d, J = 8.8 Hz, 1H), 7.63 [triplet of doublet (td), J = 7.6, 2.0 Hz, 1H], 7.55 (td, J = 7.6, 2.0 Hz, 1H), 7.21 (d, J = 8.0 Hz, 2H), 7.16 (m, 2H), 7.09 (d, J = 9.2 Hz, 2H), 6.66 (dd, J = 2.4, 8.8 Hz, 1H), 6.50 (d, J = 9.2 Hz, 2H), 6.20 (d, J = 2.0 Hz, 1H), 4.73 (m, 4H), 3.78 (s, 2H), 3.68 (m, 4H), 3.35 (m, 4 H), 3.11 (t, J = 6.0 Hz, 2H), 2.91 (s, 4 H), 2.75 (t, J = 6.0 Hz, 2H), 1.40 (t, J = 7.2 Hz, 6H). MS was performed: 816.35 calculated for $C_{45}H_{48}N_6O_9$; observed: 817.33 $(M + H)^+$, 714.42 $(M\text{-}C_4H_8NO_2)^+$, 611. 47 $(M\text{-}C_8H_{17}N_2O4)^+$, 520.45 $(M\text{-}C_{14}H_{22}N_3O_4)^+$.

ZIMIR was obtained as a red film in 18% yield: ^{1}H NMR (D_4-MeOH, 400 MHz): δ 8.33 (m, 2H), 7.86 (d, J = 8.4 Hz, 1H), 7.63 (td, J = 7.6, 2.0 Hz, 1H), 7.55 (td, J = 7.6, 2.0 Hz, 1H), 7.21–7.12 (m, 4H), 7.00 (d, J = 9.2 Hz, 2H), 6.66 (dd, J = 2.4, 8.8 Hz, 1H), 6.52 (d, J = 9.2 Hz, 2H), 6.20 (d, J = 2.0 Hz, 1H), 4.63 (m, 4H), 3.78 (s, 2H), 3.65 (m, 4H), 3.35 (m, 4H), 3.11 (t, J = 6.0 Hz, 2H), 2.90 (s, 4 H), 2.68 (t, J = 5.6 Hz, 2H), 1.84 (m, 4H), 1.38–1.10 (m, 36H), 0.88 (t, J = 7.2 Hz, 6H). MS was performed: 1,096.66 calculated for $C_{65}H_{88}N_6O_9$; observed: 854.13 $(M\text{-}C_{14}H_{28}NO_2)^+$, 611.19 $(M\text{-}C_{28}H_{57}N_2O_4)^+$, 520.24 $(M\text{-}C_{34}H_{62}N_3O_4)^+$.

Zn^{2+} Titration and Ion Selectivity of ZIMIR. To measure the Zn^{2+} affinity of ZIMIR, we performed Zn^{2+} titration of ZIMIR-C_2 (0.4 μM) using a Zn^{2+} buffering system based on nitrilotriacetic acid (NTA) (7). The buffer contained 100 mM Hepes (pH 7.5), 10 mM NTA, and varying concentrations of $ZnSO_4$ (0–9 mM) to reach a free Zn^{2+} concentration between 0.1 nM and 43 nM. Zn^{2+} concentrations above 43 nM were not buffered. However, because the commercial Hepes always contains a trace amount of divalent metal (≤5 ppm), it was necessary to add a minimum amount of NTA to chelate the residual Zn^{2+} present in the Hepes solution. We found that adding ~0.5 μM NTA to 100 mM Hepes solution was sufficient to reduce the fluorescence of ZIMIR-C_2 to the same level as seen in 43 nM (buffered) free Zn^{2+}. From that point, an increasing amount of $ZnSO_4$ was added to reach higher Zn^{2+} concentrations. Two independent Zn^{2+} titrations provided $K_d(Zn^{2+})$ values of 433 nM and 467 nM, with an average $K_d(Zn^{2+})$ of 450 nM. To examine the Zn^{2+} binding selectivity of ZIMIR against Ca^{2+} or Mg^{2+}, we measured the fluorescence intensity of ZIMIR-C_2 in a nominally Zn^{2+}-free solution containing 50 μM DPAS or in a solution containing 1 μM $ZnCl_2$ with or without Ca^{2+}/Mg^{2+} (1 mM).

1. Ravier MA, Rutter GA (2005) Glucose or insulin, but not zinc ions, inhibit glucagon secretion from mouse pancreatic alpha-cells. *Diabetes* 54:1789–1797.
2. Dakin K, Li WH (2007) Cell membrane permeable esters of D-myo-inositol 1,4,5-trisphosphate. *Cell Calcium* 42:291–301.
3. Hirano T, Kikuchi K, Urano Y, Higuchi T, Nagano T (2000) Highly zinc-selective fluorescent sensor molecules suitable for biological applications. *J Am Chem Soc* 122: 12399–12400.
4. Hauser CT, Tsien RY (2007) A hexahistidine-Zn2+-dye label reveals STIM1 surface exposure. *Proc Natl Acad Sci USA* 104:3693–3697.
5. Li DS, Yuan YH, Tu HJ, Liang QL, Dai LJ (2009) A protocol for islet isolation from mouse pancreas. *Nat Protoc* 4:1649–1652.
6. Liang HC, et al. (2005) Syntheses of water-soluble N-donor ligands for aqueous catalysis using green, Michael-type addition reactions. *Green Chem* 7:410–412.
7. Komatsu K, Kikuchi K, Kojima H, Urano Y, Nagano T (2005) Selective zinc sensor molecules with various affinities for Zn2+, revealing dynamics and regional distribution of synaptically released Zn2+ in hippocampal slices. *J Am Chem Soc* 127: 10197–10204.
8. Neuschl M, Bogdal D, Potacek M (2007) Microwave-assisted synthesis of substituted hexahydro-pyrrolo[3,2-c]quinolines. *Molecules* 12:49–59.
9. Zhang XA, Song D, Lippard SJ (2008) A reversible pH-dependent intramolecular pyridine-aldehyde cyclization. *J Org Chem* 73:734–737.

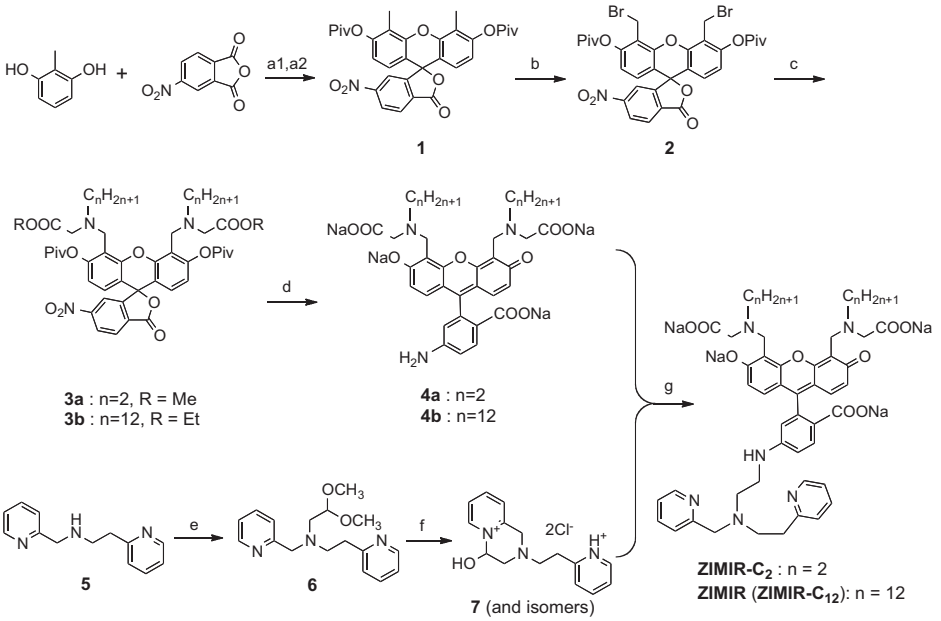

Fig. S1. Synthesis of ZIMIRs. (a1) CH_3SO_3H, reflux, 8 h. (a2) Piv_2O, Cs_2CO_3, dimethylformamide, RT, 27% for two steps. (b) N-bromosuccinimide, benzoyl peroxide, CCl_4, reflux, 4 h, 98%. (c) NaI, proton sponge, *N*-ethyl glycine methyl ester (for 3a), or *N*-dodecyl glycine ethyl ester (for 3b), CH_3CN, reflux, 14 h, 78–96%. (d) NaHS, MeOH/THF/H_2O (10:3:3), reflux, 1 h, 81% for 4a and 74% for 4b. (e) 2-Bromo-1,1-dimethoxyethane, KF/celite (1:1), CH_3CN, reflux, 3 d, 60%. (f) 1 M HCl, 5 h, 99%. (g) $NaBH_3CN$, Na_2SO_4, RT, overnight, 36% for ZIMIR-C_2 and 18% for ZIMIR.

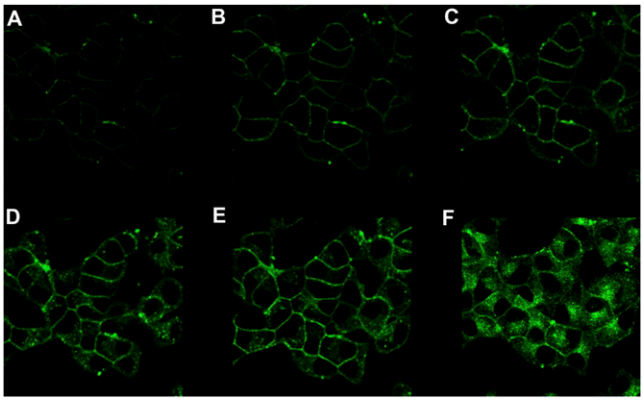

Fig. S2. ZIMIR labels plasma membranes of intact living cells rapidly, noninvasively, and stably. ZIMIR (1 μM) was added to MIN6 cells in HBS buffer (containing ~1 μM Zn^{2+} to enhance fluorescence intensity). Confocal images (Ex, 488 nm; Em, 510–550 nm) were subsequently acquired at 2 min (*A*), 5 min (*B*), 10 min (*C*), and 20 min (*D*). Cells were then washed with HBS buffer three times and imaged again at 21 min (*E*) and 140 min (*F*). Scale bar, 20 μm.

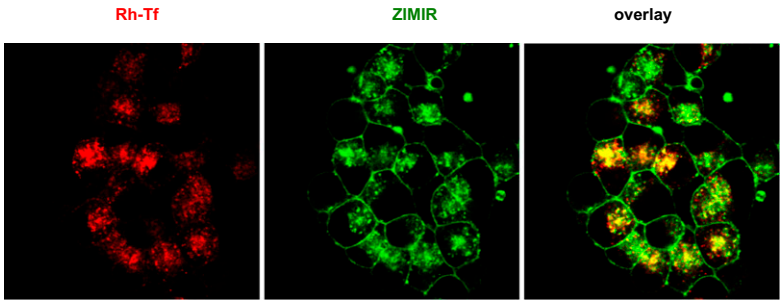

Fig. S3. Intracellular staining of rhodamine-transferrin (Rh-Tf) overlaps with that of ZIMIR. MIN6 cells were labeled with ZIMIR (1 μM) and Rh-Tf (20 μg/mL; Invitrogen) in serum-free DMEM at 37 °C for 30 min. Cells were then washed and imaged 15 min later. Scale bar, 10 μm.

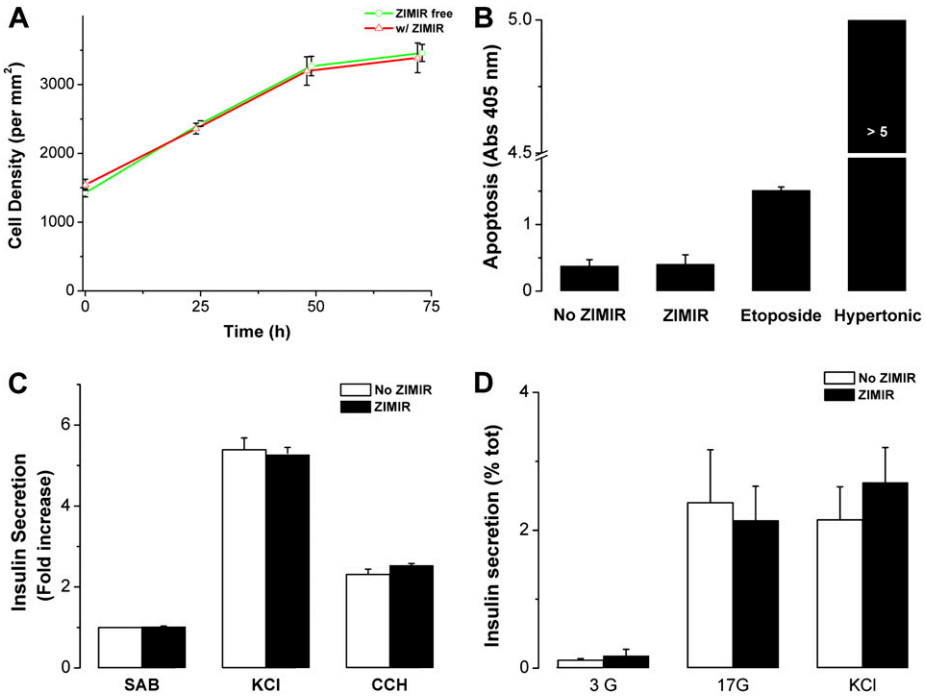

Fig. S4. ZIMIR labeling had little effect on β cell growth, cell death, or insulin secretion. (*A*) Growth of ZIMIR-labeled MIN6 cells was identical to that of control unlabeled cells. Cells in a 35-mm dish were labeled with ZIMIR (1 μM) in SAB buffer for 30 min, washed, and cultured for the next 3 d. Cells were counted every 24 h. (*B*) Cell death after ZIMIR labeling showed little difference from that in control unlabeled cells. Cells were labeled with ZIMIR (1 μM) in SAB buffer for 30 min, washed, and incubated in the culture medium for another 2 h before apoptosis was assayed using the Cell Death Detection Elisa kit (Roche Applied Science) by measuring the absorption at 405 nm (Abs 405 nm). Positive controls for apoptosis included DNA topoisomerase inhibitor etoposide (0.5 mM, 2.5 h) and hypertonic shock [10 mM Tris (pH 7.4), 400 mM NaCl, 5 mM $CaCl_2$, and 10 mM $MgCl_2$ for 2 h]. Abs. (*C*) ZIMIR labeling did not affect insulin secretion in cultured MIN6 cells. MIN6 cells were stimulated with 40 mM KCl or 0.25 mM carbachol (CCH) for 30 min at 37 °C. The amount of released insulin (Insulin ELISA; Calbiotech) was normalized against control MIN cells bathed in SAB buffer with 3 mM glucose. (*D*) ZIMIR labeling did not affect insulin secretion in mouse islets. CD1 mouse islets in 12-well plates (6 islets per well) were incubated for 30 min in 0.5 mL of Krebs buffer with 3 mM glucose at 37 °C. Subsequently, islets were stimulated for a further 30 min with either 3 mM glucose (3G), 16.7 mM glucose (17G), or 30 mM KCl. Both the released insulin and the total insulin content were measured, and the percent of insulin secretion was calculated against total insulin content (% tot). n = 3 for all the measurements.

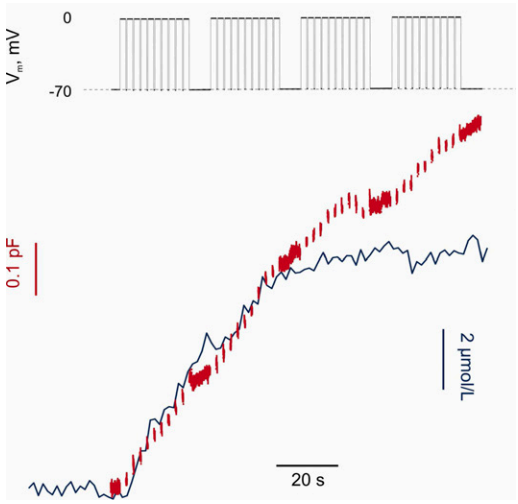

Fig. S5. Depolarization-induced changes in membrane capacitance coincide with increase in ZIMIR fluorescence. The cell was held at a plasma membrane potential (V_m) of −70 mV (black, *Upper*), and several trains of depolarizations were applied. Each train consisted of ten 2.5-s pulses to 0 mV separated by 0.5-s repolarizations to −70 mV (*Upper*). (*Lower*) Sinusoid (30 mV, 500 Hz) was applied during the repolarizations, which allowed measurement of electrical capacitance (red). ZIMIR fluorescence (blue) was recorded simultaneously and calibrated to extracellular Zn^{2+} concentration. The calibration was done by application of the extracellular solution with the Zn^{2+} concentration buffered by diluting 1 mM $ZnCl_2$ stock in the extracellular solution containing 100 μM EDTA. The total Zn^{2+} required for 0.01 μM, 0.1 μM, 1 μM, and 10 μM free Zn^{2+} concentrations was calculated using Maxchelator (Chris Patton, Stanford University).

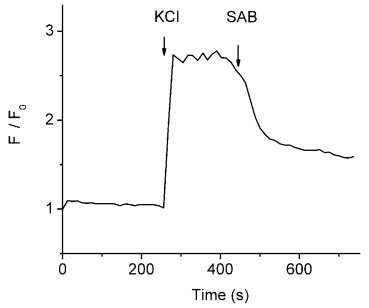

Fig. S6. ZIMIR signal remained elevated after termination of KCl stimulation. After KCl (40 mM) stimulation, MIN6 cells were washed with the SAB containing 5 mM KCl. EDTA (10 μM) was present throughout the experiment. F, fluorescence.

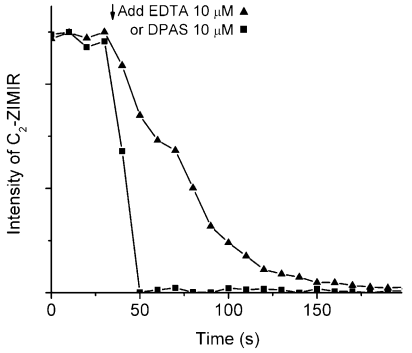

Fig. S7. DPAS chelates Zn^{2+} much faster than EDTA. In this competition assay, fluorescence intensity (excitation, 490 nm; emission, 525 nm) of ZIMIR-C_2 (1 μM) in HBSS was recorded. The rate of fluorescence intensity decline after adding EDTA or DPAS reflects the kinetics of EDTA/Zn^{2+} or DPAS/Zn^{2+} complexation.

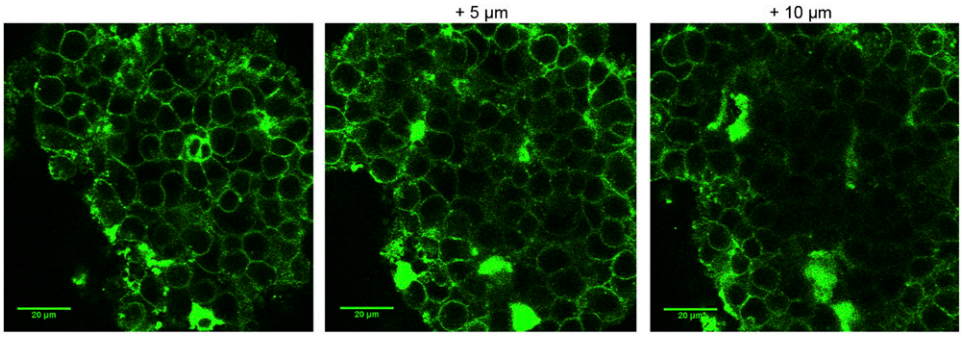

Fig. S8. ZIMIR rapidly labels cells of intact human islets. Representative CLSM images of a ZIMIR-labeled human islet at three focal planes 5 μm apart.

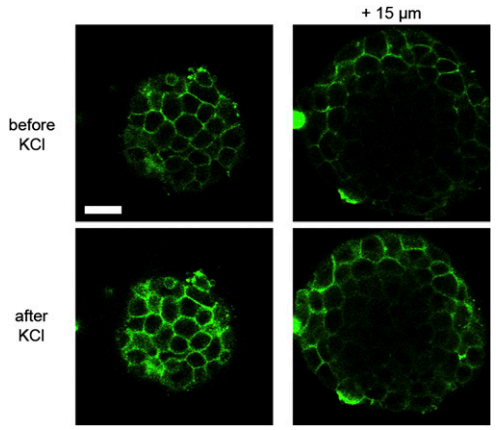

Fig. S9. Confocal ZIMIR imaging of insulin/Zn^{2+} release in a mouse islet bathed in SAB. Images from two example layers 15 μm apart before and 10 s after KCl (40 mM) stimulation are shown. The images correspond to Movie S7. Scale bar, 20 μm.

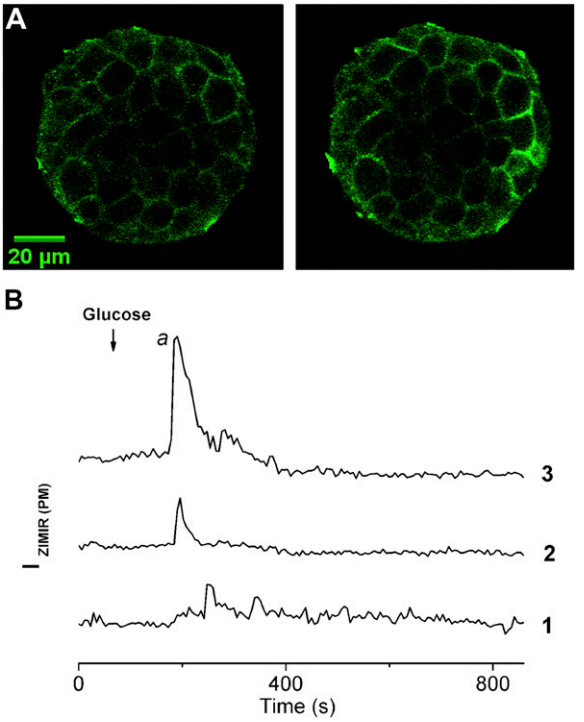

Fig. S10. ZIMIR imaging of GSIS in intact islets. (*A*) Confocal ZIMIR images of an islet before (*Left*) and after (*Right*) 20 mM glucose stimulation (corresponding to time point *a* in *B*). (*B*) Time courses of ZIMIR fluorescence of three example regions of interest (indicated in *A*). The images correspond to Movie S10. Scale bar, 20 μm.

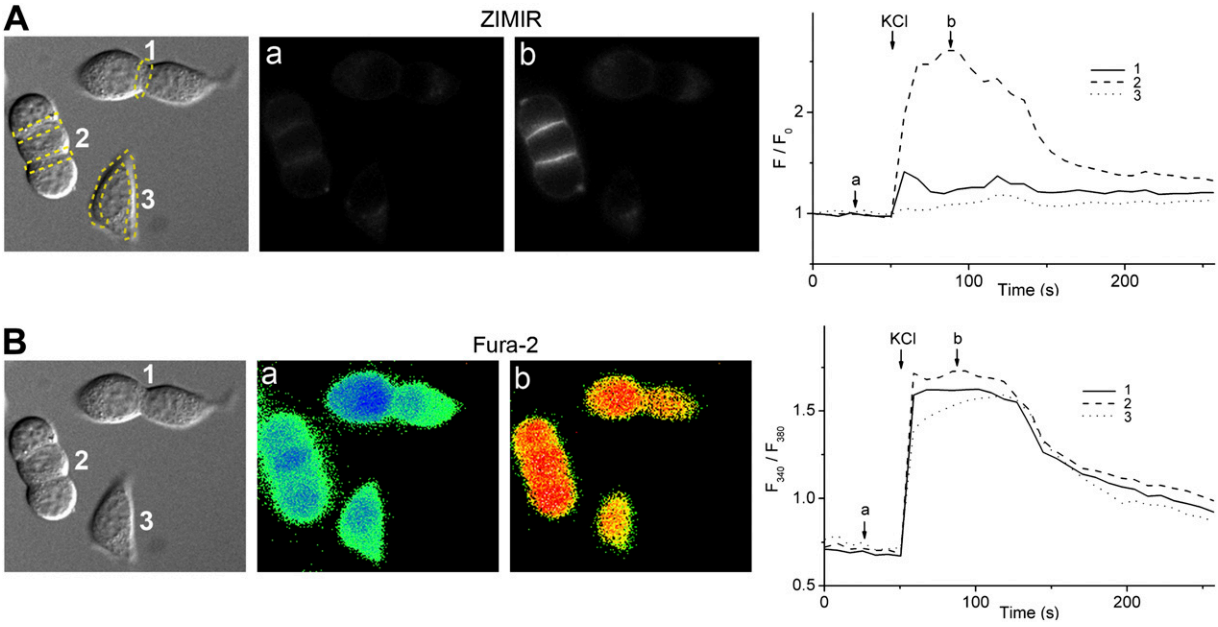

Fig. S11. Concurrent imaging of insulin/Zn^{2+} release and $[Ca^{2+}]_c$ in MIN6 β cells. Example ZIMIR fluorescence images (*A*) and Fura-2 pseudocolor ratio images (*B*) (340-nm vs. 380-nm excitation) corresponded to time points a and b marked on the time courses. ZIMIR intensity changes were plotted for three regions of interest, marked as dashed circles in the DIC image, and corresponded to the cell-cell contact of a cell doublet (1), the average of cell-cell contacts of a cell triplet (2), and along the plasma membrane of a singlet (3), respectively. Corresponding Fura-2 ratio changes were measured in the bulk cytosol of these three areas. F, fluorescence.

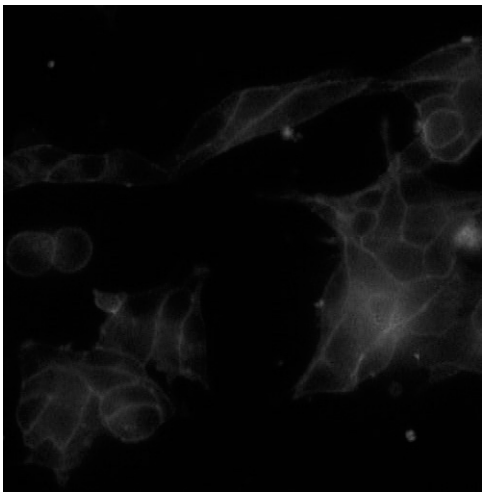

Movie S1. ZIMIR rapidly and noninvasively labels cell membranes of intact living cells. ZIMIR (1 μM) was added to MIN6 cells bathed in HBSS containing 20 mM Hepes (pH 7.3) and 5 mM glucose. Images were acquired every 30 s for ~20 min.

Movie S1

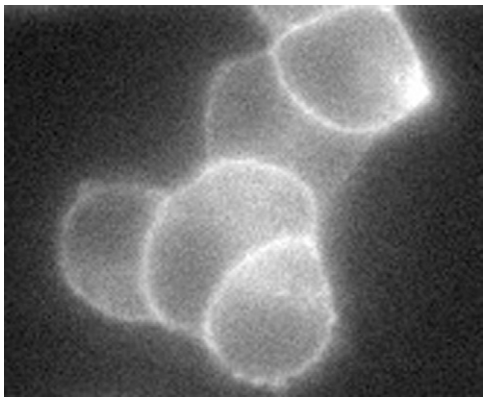

Movie S2. ZIMIR imaging of KCl (40 mM)-stimulated insulin/Zn^{2+} release in MIN6 cells. Time courses of membrane ZIMIR changes are shown in Fig. 3*E*.

Movie S2

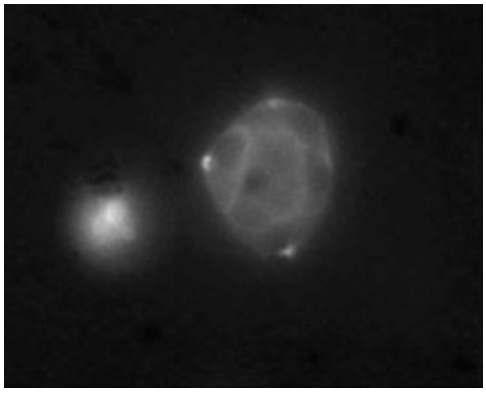

Movie S3. ZIMIR imaging of insulin/Zn^{2+} release in primary β cells from a WT mouse (C57BL/6). Time courses of membrane ZIMIR changes are shown in Fig. 3*F*.

Movie S3

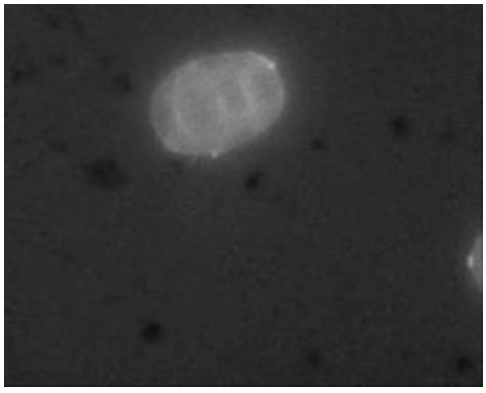

Movie S4. ZIMIR imaging of insulin/Zn^{2+} release in primary β cells from a *Znt8* KO mouse (C57BL/6). Time courses of membrane ZIMIR changes are shown in Fig. 3*G*.

Movie S4

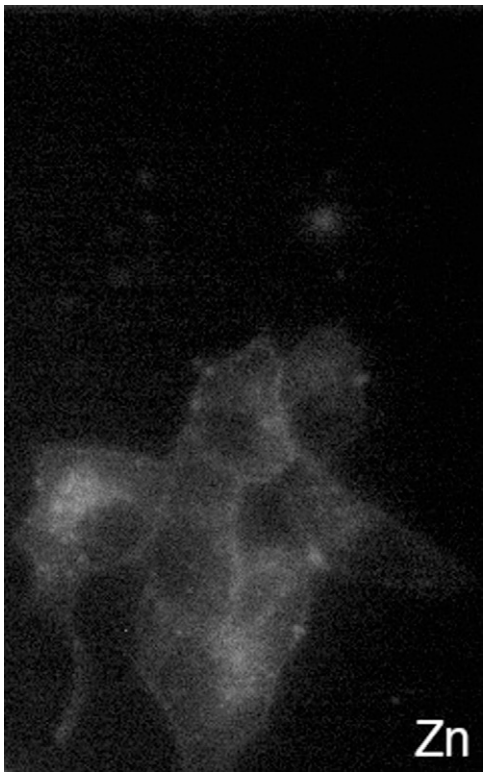

Movie S5. ZIMIR imaging of oscillatory insulin/Zn^{2+} release in MIN6 cells. Time courses of membrane ZIMIR changes are shown in Fig. 4*B*.

Movie S5

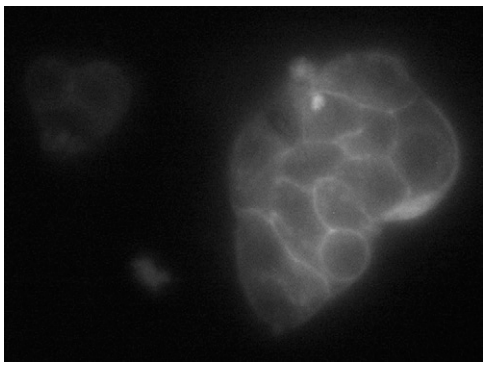

Movie S6. ZIMIR imaging of pulsatile insulin/Zn^{2+} release in primary β cells from human islets. Images were acquired every 4 s for ~12.5 min.

Movie S6

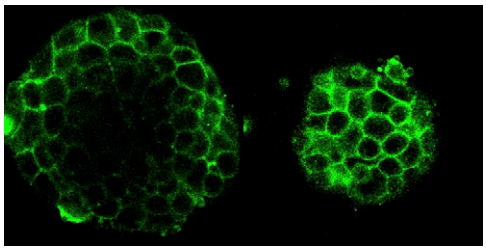

Movie S7. CLSM of insulin/Zn^{2+} release in a mouse islet on KCl stimulation. Images were acquired every 6 s for ~6 min. The two confocal layers were 15 μm apart.

Movie S7

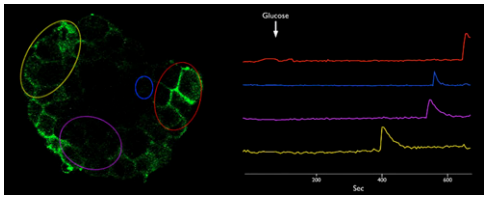

Movie S8. CLSM of GSIS in a rat islet (Sprague–Dawley). Four clusters of β cells, highlighted by colored circles at the beginning and end of the movie, showed strong ZIMIR responses at different times after glucose challenge. Time courses of their corresponding ZIMIR fluorescence changes are shown as an animated plot to the right (also as in Fig. 6*B*).

Movie S8

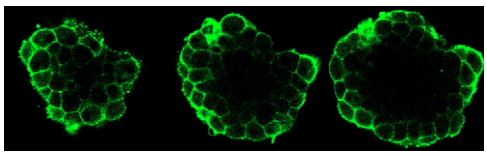

Movie S9. CLSM of GSIS of the same rat islet shown in Movie S8. Images from three confocal layers 10 μm apart are shown. Images of middle layer are the same as in Movie S8.

Movie S9

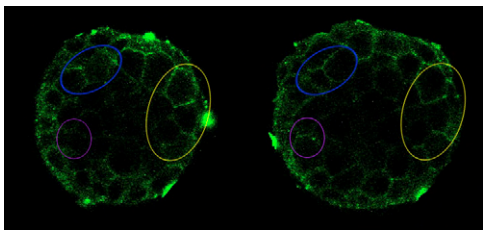

Movie S10. CLSM of synchronized GSIS among several clusters of β cells in a rat islet (Sprague–Dawley). Time courses of the corresponding ZIMIR fluorescence changes are shown in Fig. S10.

Movie S10

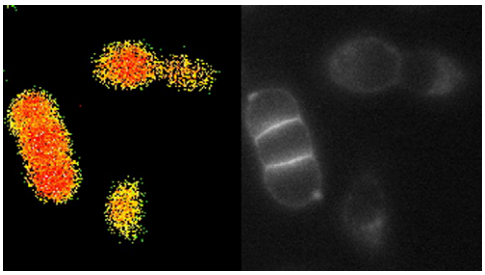

Movie S11. Dual-color imaging of ZIMIR and Fura-2 in MIN6 cells. Time courses of ZIMIR and Fura-2 changes are plotted in Fig. S11.

Movie S11